Accepted Manuscript

Bio- and hydrochars from rice straw and pig manure: Inter-comparison

Yuxue Liu, Shuai Yao, Yuying Wang, Haohao Lu, Satinder Kaur Brar, Shengmao Yang

Please cite this article as: Liu, Y., Yao, S., Wang, Y., Lu, H., Kaur Brar, S., Yang, S., Bio- and hydrochars from rice straw and pig manure: Inter-comparison, *Bioresource Technology* (2017), doi: http://dx.doi.org/10.1016/j.biortech.2017.03.103

1 **Bio- and hydrochars from rice straw and pig manure: Inter-comparison**

2 Yuxue Liu[a,b], Shuai Yao[c], Yuying Wang[a,b], Haohao Lu[a,b], Satinder Kaur Brar[d], Shengmao Yang [a,b,*]

3 [a]*Institute of Environment, Resource, Soil and Fertilizer, Zhejiang Academy of Agricultural Sciences, 198 Shiqiao Road, Hangzhou 310021,*

4 *China*

5 [b]*Engineering Research Center of Biochar of Zhejiang Province, Hangzhou 310021, China*

6 [c]*College of Environment, Zhejiang University of Technology, Hangzhou 310014, China*

7 [d]*INRS-ETE, Université du Québec, 490, Rue de la Couronne, Québec G1K 9A9, Canada*

8

9 [*]Corresponding author. E-mail: yangshengmao@263.net; tel.: +86 571 8641 9218; fax: +86 571 8641 9218.

10

1

11 **Abstract:** Conversion of rice straw (RS) and pig manure (PM) into chars is a promising disposal/recycling option. Herein, pyrolysis and

12 hydrothermal carbonization were used to produce bio- and hydrochars from RS and PM, affording lower biochar (300–700 ℃) and hydrochar

13 (180–300 °C) yields at higher temperatures within the specified range. The C contents and C/N ratios of RS chars were higher than those of PM

14 ones, with the opposite trend observed for yield and ash content. C and ash contents increased with increasing temperature, whereas H/C, O/C,

15 and (O+N)/C ratios decreased. The lower H/C ratio of biochars compared to that of hydrochars indicated greater stability of the former. KCl was

16 the main inorganic fraction in RS biochars, whereas quartz was dominant in PM biochars, and albite in PM hydrochars. Thus, RS is more

17 suitable for carbon sequestration, while PM is more suitable for use as a soil amendment substrate.

18 **Keywords:** biowaste; biochar; hydrochar; pyrolysis; hydrothermal carbonization

19

1 Introduction

Rice is a staple food for more than 3.5 billion people worldwide, i.e., for around half of the world population. In 2008, about 620 million tons of

rice straw was produced in Asia alone, with this quantity increasing every year. In most places, this waste has no commercial value and is

disposed of in various ways. Rice straw contains about 0.6% (w) N, 0.1% P and S (each), 1.5% K, 5% Si, and 40% C (Ponnamperuma, 1984),

being a convenient source of plant nutrients due to its on-the-spot availability in amounts varying from 2 to 10 t/ha. Although residue retention is

essential for the sustainable soil management of non-rice crops and mixed cropping (rice-upland crops), direct incorporation of rice straw into

soil usually causes methane emissions due to its anaerobic breakdown. The alternative (where practiced) burning of rice straw in fields results in

airborne emissions hazardous to humans and the ecosystem. Therefore, the development of a proper rice straw treatment method preceding its

incorporation into soil is urgently required.

Moreover, another important issue concerns waste management in the livestock industry. Livestock production, mainly comprising pig and

poultry farming, has developed rapidly in China, especially after the launch of economic reforms (Zheng et al., 2014). The intensive industrial

livestock production has resulted in a high density of animals in relatively small areas, with large quantities of manure produced in recent years

(Ko et al., 2008). As a result, the nitrogen- and phosphorus-containing manure constituents contaminate soil and water bodies, also resulting in

33 odor pollution, particularly in and around production buildings, storage areas, and during pig manure spreading (Makara and Kowalski, 2015).

34 Therefore, the need for more environmentally friendly methods for the treatment and utilization of pig manure has become imperative, making

35 the significance of establishing an integrated crop-livestock system hard to overstate.

36 Biochar refers to carbon-rich solid particles produced from biomass by pyrolysis under oxygen-limited conditions at a relatively low temperature

37 (< 700 °C) (Chen et al., 2008; Lehmann, 2007), typically exhibiting a well-developed pore structure, very large surface area, high stability, and

38 exceptional adsorption properties (Kei et al., 2004). The increasing attention enjoyed by biochar in recent years is ascribed to its beneficial use

39 for carbon sequestration, climate change mitigation, soil amendment, and contaminant removal (Chan et al., 2007; Mohan et al., 2014; Tan et al.,

40 2015). Hydrochar refers to the solid products of hydrothermal carbonization, which is a promising alternative waste management strategy for

41 biomass residuals, especially those with high water content (up to 80%) (Catalkopru et al., 2017). In terms of structure, hydrochar is closer to

42 coal than biochar produced by dry pyrolysis (Berge et al., 2013), being potentially suitable for a wide range of applications such as carbon

43 sequestration, adsorbents, container nurseries, fuels, and even soil additives (Guo et al., 2015). Extensive efforts have been directed at the

44 production of energy-rich hydrochars from a wide range of lignocellulosic biomasses, digestate, and manure. Generally, the characteristics of

45 bio- and hydrochars mainly depend on the type of feedstock and pyrolysis/carbonization processes. However, the effects of

4

46   pyrolysis/carbonization conditions on the properties of bio-/hydrochars derived from the same biomass are yet to be thoroughly assessed.

47   Therefore, in the present work, rice straw and pig manure were chosen as pyrolysis and hydrothermal carbonization precursors, and the

48   corresponding bio- and hydrochars were produced under a series of thermal conditions. The characteristics of these chars were determined to

49   investigate the differences between the above thermochemical processes at various temperatures, as well as those between rice straw and pig

50   manure. Thus, this study provides a basis for the disposal and utilization of biowaste produced by agriculture and the livestock industry.

51

52   **2 Materials and methods**

53   **2.1 Preparation of bio- and hydrochars**

54   Rice straw (RS) and pig manure (PM) were collected as raw biomasses and used to produce bio- and hydrochars utilizing two types of

55   thermochemical processes. RS was collected from Haining City, Zhejiang Province, China, shredded into pieces of less than 5 mm, and air-dried.

56   The compositional analysis of RS yielded the following results: cellulose 38.2 wt%, hemicellulose 20.1 wt%, and lignin 21.4 wt%. PM was

57   collected from Tongxiang City, Zhejiang Province, China, and also air-dried. The dried RS and PM samples were sealed in a plastic container for

58   further use.

5

59 Pyrolysis was performed in a programmable tube furnace (Hangzhou Lantian Instrument Co., Ltd., China), whose schematic is shown in Fig. 1.

60 Typically, the prepared biomass was slowly pyrolyzed under anaerobic conditions at a heating rate of 25 °C min^{-1} and a residence time of 1.5 h.

61 Final temperatures of 300, 500, and 700 °C were used, and the produced biochars were allowed to cool to room temperature after pyrolysis.

62 Hydrothermal carbonization was performed in a 2-L stainless steel pressure reactor, as shown in Fig. 2. The reaction temperature was controlled

63 at 180, 240, and 300 °C by a single-display proportional – integral – derivative (PID) controller. In this temperature range, biomass components

64 become more reactive: hemicellulose is degraded at ~200 °C, cellulose starts to react above 230 °C, and lignin is partially decomposed above

65 260 °C (Funke and Ziegler, 2010). For each run, 50 g of RS or 150 g of PM and 1 L of distilled water were loaded into the reactor, heated to the

66 desired temperature at 3 °C min^{-1}, and held at the final temperature for 1.5 h. During the process, the mixture of water and biomass was

67 continuously stirred by a magnetic stirrer at 150 rpm to ensure uniform heating. After 1.5 h, the reactor was allowed to air-cool, and the gaseous

68 products were released into the atmosphere. The solid and liquid products were separated by gravity filtration using 150-mm qualitative filter

69 circles. The obtained hydrochar samples were air-dried in a ventilated fume cupboard for 48 h.

70 For simplicity, the bio-/hydrochars derived from RS were denoted as RS-P300, RS-P500, RS-P700, RS-H180, RS-H240, and RS-H300, and

71 those derived from PM were denoted as PM-P300, PM-P500, PM-P700, PM-H180, PM-H240, and PM-H300, where the letters P/H stand for

6

72 pyrolysis/hydrothermal carbonization, respectively, and the numbers represent the final temperature. All biochars were milled to a homogenous

73 fine powder using a ball mill and dried overnight at 105 °C prior to being analyzed.

74 **2.2 Analytical methods**

75 Yields of bio- and hydrochars were calculated as fractions of raw material mass, and the char properties, such as pH, were investigated at a

76 solid:water ratio of 1:20 (w/v). The suspension was first shaken and equilibrated for 5 min, and pH measurements were performed in triplicate

77 using a pH meter (Mettler-Toledo, Switzerland). Electric conductivity (EC) was measured by an EC meter. The moisture content of chars was

78 determined from the sample mass loss at 105 °C, whereas ash and volatile matter contents were calculated from the residual weight obtained

79 after heating at 815±1 °C for 2 h and 900±1 °C for 7 min, respectively, in a muffle furnace (National Standard of the People's Republic of China,

80 GB/T 212-2008). Fixed carbon content was calculated by subtracting the ash and volatile matter content from 100% on a dry basis. C, H, N, and

81 S contents of bio- and hydrochars were determined using an elemental analyzer (Vario EL/micro cube, Elementar, Germany). The oxygen

82 content was calculated by subtracting C, N, H, S, and ash contents from the total char mass. The specific surface area, total pore volume, and

83 mean pore size of biochar were measured with a BET surface area analyzer (ASAP2020, Micromeritics, USA) using N_2 adsorption. Inorganic

84 components of chars were identified based on their X-ray diffraction (XRD) patterns obtained using an X-ray diffractometer (D8 Advance,

7

85 Bruker, Germany) equipped with a graphite-monochromatized Cu K_{α} radiation source (λ = 1.541841 Å) and employing a scan rate of 0.01° s^{-1} in

86 a 2θ range of 10–70°. The surface functional groups of biochars were characterized by Fourier transform infrared (FTIR) spectroscopy (Varian

87 640-IR, USA) in a wavelength range of 400–4000 cm^{-1} using KBr pellets at room temperature. SigmaPlot 10.0 software was used for drawing

88 figures.

89

90 **3 Results**

91 **3.1 Basic physical and chemical properties of bio- and hydrochars**

92 The yields, atomic ratios, pH, ECs, specific surface areas, total pore volumes, and mean pore sizes of bio- and hydrochars derived from RS and

93 PM at different temperatures are listed in Table 1, whereas their elemental compositions and ash contents are shown in Fig. 3. For each feedstock,

94 higher temperatures resulted in lower bio-/hydrochar yields, which equaled 25.6–57.7% for RS and 38.0–57.8% for PM. At the same

95 temperature, the yields of PM-derived bio-/hydrochars were higher than those of RS-derived chars. The ash contents of RS- and PM-derived bio-

96 and hydrochars increased with increasing temperature, equaling 24.4–42.8% and 6.59–35.4% for chars obtained by pyrolysis and hydrothermal

97 carbonization, respectively. The ash contents of PM-derived bio- and hydrochars were higher than those of RS-derived chars under the same

8

98 conditions. The C contents of bio- and hydrochars derived from both RS and PM increased with increasing temperature, whereas their H and O

99 contents, as well as H/C, O/C, and (O + N)/C ratios decreased. For each feedstock, the C/N ratio of biochar increased with increasing

100 temperature, while it decreased for hydrochar. The C contents and C/N ratios of bio-/hydrochars derived from RS (44.1–61.7% and 51.8–91.4,

101 respectively) were much higher than those of PM-derived chars (43.3–46.4% and 18.0–39.4, respectively) at the same temperature. Furthermore,

102 the H/C ratios of hydrochars derived from both RS (0.94–1.47) and PM (0.91–1.18) were higher than those of RS- and PM-derived biochars

103 (0.37–1.04 and 0.31–1.00, respectively).

104 The pH of RS- and PM-derived biochars increased with increasing temperature, equaling 7.15–10.6 for thermal treatment temperatures of

105 300–700 °C (Table 1). A similar tendency was observed for the pH of hydrochars derived from RS and PM (except for RS-H180), which equaled

106 5.43–5.99 at 180–300 °C. The ECs of both RS- and PM-derived biochars increased with increasing temperature, with RS-derived biochar

107 exhibiting much higher values (4.36–5.89 mS cm^{-1}) than PM-derived biochar (0.543–0.919 mS cm^{-1}). Conversely, the ECs of hydrochars

108 decreased with increasing temperature, with PM-derived hydrochar (0.051–0.147 mS cm^{-1}) exhibiting higher values than RS-derived hydrochar

109 (0.040–0.062 mS cm^{-1}).

110 The specific surface areas of most bio- and hydrochars were very low (2.57–32.9 m^2 g^{-1}, Table 1). Under pyrolytic conditions, the specific

9

111 surface areas and total pore volumes of RS- and PM-derived biochars increased with increasing temperature, whereas their mean pore sizes

112 decreased. The specific surface area of RS-derived biochar (3.35–32.9 $m^2\ g^{-1}$) was higher than that of PM-derived biochar (3.32–20.5 $m^2\ g^{-1}$),

113 and the mean pore size of RS-derived biochar (59.2–151.3 nm) was lower than that of PM-derived biochar (88.4–229.9 nm). However, the

114 specific surface areas, total pore volumes, and mean pore sizes of RS- and PM-derived hydrochars exhibited an initial increase and a subsequent

115 decline with increasing temperature. The specific surface area and total pore volume of PM-derived hydrochar (10.7–15.6 $m^2\ g^{-1}$ and

116 0.0728–0.1212 cm^3/g, respectively) were higher than those of RS-derived hydrochar (2.57–4.46 $m^2\ g^{-1}$ and 0.0128–0.0382 cm^3/g, respectively).

117 **3.2 Composition of char ash determined by XRD**

118 Typical XRD patterns of bio- and hydrochars are shown in Fig. S1 (Supplementary data). For RS-derived biochars, sylvite (KCl) and quartz

119 (SiO_2) were the main crystalline phases detected after pyrolysis at 300 °C, with calcite ($CaCO_3$) also detected at temperatures above 500 °C. For

120 PM-derived biochars, $CaCO_3$ and SiO_2 were the major inorganic crystalline phases observed at 300 °C, with magnesium silicate ($MgSiO_3$)

121 detected at 500 °C, and dolomite [$CaMg(CO_3)_2$] and albite ($NaAlSi_3O_8$) observed at 700 °C. Furthermore, only small amounts of crystalline

122 phases were detected at 180–300 °C for RS-derived hydrochars. In contrast, SiO_2 and $NaAlSi_3O_8$ were the main inorganic crystalline phases

123 observed at 180–300 °C for PM-derived hydrochars, with $CaCO_3$ observed at 240 °C and [$CaMg(CO_3)_2$] detected at 300 °C.

10

3.3 Surface property analysis by FTIR

Functional groups of bio- and hydrochars were analyzed by FTIR spectroscopy, with the obtained spectra presented in Fig. S2 (Supplementary data). For RS-derived biochars, the intensity of peaks at 3397, 2920, 1110, and 789 cm^{-1} decreased with increasing temperature, and some peaks disappeared at 700 °C. For PM-derived biochars, peaks at 3397, 2920, 2358, 1092, and 769 cm^{-1} were well preserved at 300 and 500 °C, but lost intensity at 700 °C, whereas peaks at 1591 and 1350 cm^{-1} exhibited an intensity decrease with increasing temperature. Conversely, for both RS- and PM-derived hydrochars, peaks at 2928, 2360, 1600 and 800 cm^{-1} became sharper with increasing temperature, and those at 2850 and 1114 cm^{-1} appeared at 300 °C for RS-derived hydrochars.

4 Discussion

4.1 Basic characteristics of bio- and hydrochars

During thermochemical processing, the char yield (defined as the mass ratio of dry bio-/hydrochar to that of input dry feedstock) usually decreases with increasing temperature due to the formation of liquid and gaseous by-products (Libra et al., 2011). The reduced yields of RS- and PM-derived bio-/hydrochars with increasing treatment temperature (Table 1) are mainly associated with the removal of cellulosic and

11

137   hemicellulosic components (Kambo and Dutta, 2015).

138   The high ash content of individual bio-/hydrochars directly correlates with yield reduction. For both RS and PM, the ash content of biochar was

139   usually higher than that of hydrochar at the same treatment temperature (Fig. 3), in agreement with the results of Dai et al. (2015), who

140   concluded that hydrothermal carbonization can be employed to dissolve and wash out some inorganic components from hydrochar.

141   As reported in numerous previous researches (Chen et al., 2008; Ghanim et al., 2016; Keiluweit et al., 2010; Smith et al., 2016), thermal

142   treatment temperature is the primary factor determining bio-/hydrochar properties. Elevated temperatures favored higher C contents, which

143   increased for all bio-/hydrochars produced from RS and PM (Fig. 3). Conversely, H and O contents markedly decreased with increasing

144   temperature, indicating the occurrence of decarboxylation, decarbonylation, and dehydration during pyrolysis and hydrothermal carbonization of

145   biomass (Ghanim et al., 2016). The H/C atomic ratio was proposed as an index of aromaticity and resistance of bio-/hydrochars to microbial and

146   chemical degradation (Crombie et al., 2013). This ratio significantly decreased with increasing temperature for all chars, suggesting an increase

147   of their aromaticity. The lower H/C ratio of biochar compared to hydrochar indicates the greater stability of the former.

148   The decrease of the polarity index (O + N)/C and the O/C atomic ratio with increasing temperature indicated a reduction of polarity and the

149   number of oxygen-containing functional groups. This agrees with previous reports, suggesting that pyrolysis and hydrothermal carbonization of

150 biomass result in removal of hydroxyl groups via dehydration, loss of carboxyl and carbonyl groups via decarboxylation, cleavage of ester and

151 ether bonds via hydrolysis, and, for lignocellulose-based biomass, in increased aromatization due to the dehydration of lignin and aromatization

152 of carbohydrates (Funke and Ziegler, 2010; Smith et al., 2016).

153 It should be noted that bio-/hydrochar properties varied greatly with biomass type. The C content of RS-derived bio-/hydrochars was much

154 higher and exhibited a more obvious increase upon pyrolysis than that of PM-derived ones (Fig. 3), indicating that RS is more suitable for

155 carbon sequestration than PM. Similar to the C content, the O content of RS-derived bio-/hydrochars markedly decreased with temperature.

156 Unlike RS, PM is a sort of livestock manure, commonly containing a large number of inorganic elements (e.g., K, Ca). PM contains abundant

157 porcine metabolites, being easily decomposable in comparison to plant biomass. The C/N ratio of RS-derived bio-/hydrochars was much higher

158 than that of PM-derived ones (Table 1), indicating that PM is more suited for use as a soil amendment substrate than RS, since an overly high

159 C/N ratio that goes against decomposition by microbes will result in excessive consumption of available soil nitrogen.

160 **4.2 Composition of bio- and hydrochars**

161 XRD was used to detect the short-range ordered structures of bio- and hydrochars and the crystalline structures of the present minerals (Wang et

162 al., 2016). The observed strong and sharp peaks indicated the presence of crystalline inorganic phases in bio- and hydrochars derived from RS

163 and PM. The speciation and abundance of inorganic constituents were determined by thermal treatment temperature and feedstock properties.

164 Under the same conditions, the peaks of RS-derived bio- and hydrochars were less abundant than those of PM-derived chars, indicating the

165 lower ash content of the former and being in agreement with the results presented in Table 1. For example, the weak peaks observed for

166 RS-derived hydrochars demonstrated their low inorganic content, whereas quartz and albite were detected in PM-derived hydrochars. Peaks at

167 28° and 41° confirmed the presence of sylvite in RS-derived biochars, whereas those at 27° were indicative of quartz in PM-derived biochars.

168 In addition, the results showed that a larger amount of crystalline inorganic fractions was formed in both RS and PM at high temperatures during

169 pyrolysis and hydrothermal carbonization. For RS-derived biochars, the peak of calcite at 29° was observed only above 500 °C. In contrast, for

170 PM-derived biochars, peaks at 28°, 31°, 36°, and 43° indicated that $MgSiO_3$ was formed above 500 °C, and albite (22° and 28°) and dolomite

171 (31° and 41°) were formed at 700 °C. For PM-derived hydrochars, the peak at 29° confirmed the formation of calcite during hydrothermal

172 carbonization at 240 °C, and that at 31° was due to the formation of dolomite at 300 °C.

173 Li et al. (2017) found that the type and amount of inorganic crystalline phases in biochar depend on the feedstock and temperature. However,

174 their results demonstrated that KCl formed at relatively low pyrolysis temperature (200–300 °C), while carbonates generally formed above

175 400 °C.

14

4.3 Surface property of bio- and hydrochars

As demonstrated by the FTIR spectra, the band at 3397 cm^{-1}, attributed to the stretching vibrations of hydrogen-bonded hydroxyl groups of water (Droussi et al., 2009), lost intensity with increasing temperature and disappeared at 700 °C for both RS- and PM-derived biochars. For all biochars, peaks at 2920, 2850, and 1458 cm^{-1} (aliphatic CH$_2$) (Xiao et al., 2014) gradually disappeared with increasing temperature. The intense bands of aromatic C=C and C=O groups (1591–1601 cm^{-1}) (Chun et al., 2004) were well preserved between 180 and 500 °C, but lost intensity at 700 °C in the case of PM-derived biochar. Peaks of aliphatic C–O–C fragments at 1092–1114 cm^{-1} (Li et al., 2017) disappeared at temperatures above 500 °C for PM-derived biochar, being better preserved for RS-derived biochar. Peaks observed at 3397, 2920, 2850, 1591, 1458, 1355, and 1100 cm^{-1} indicated that a large number of organic residues (e.g., polymeric –CH$_2$–, fatty acids, lignins, and polysaccharides) were preserved in RS- and PM-derived hydro- and biochars at low temperature (300 °C), whereas some of them disappeared in biochars pyrolyzed at high temperature, e.g., above 500 °C. The changes observed in the range of 1000–1400 cm^{-1} (C–O) and at 1591 cm^{-1} (C=O) indicated that oxygen-containing functional groups might have been oxidized during hydrothermal carbonization and pyrolysis.

5 Conclusions

15

189 High temperature resulted in lower bio-/hydrochar yields. C and ash contents increased with increasing temperature, while H/C, O/C, and

190 (O+N)/C ratios decreased. Higher C contents and C/N ratios of RS chars compared to those of PM chars indicate that RS is more suitable for

191 carbon sequestration, whereas PM is suitable for soil amendment. Biochars showed lower H/C ratios than hydrochars due to their greater

192 stability. KCl was the main inorganic fraction in RS biochars, while SiO_2 was dominant in PM biochars, and $NaAlSi_3O_8$ was detected in PM

193 hydrochars. The number of surface groups in biochars gradually decreased with increasing temperature.

194

195 **Acknowledgements**

199

200 **References**

201 [1] Berge, D.N., Kammann, C., Ro, K., Libra, J., 2013. Environmental applications of hydrothermal carbonization technology: biochar

202   production, carbon sequestration, and waste conversion. In: Titirici, M.M. (Ed.), Sustainable Carbon Materials from Hydrothermal Processes.

203   John Wiley & Sons, Ltd., United Kingdom, p. 297.

204 [2] Catalkopru, A.K., Kantarli, I.C., Yanik, J., 2017. Effects of spent liquor recirculation in hydrothermal carbonization. Bioresour. Technol. 226,

205   89–93.

206 [3] Chan, K.Y., Van Zwieten, L., Meszaros, I., Downie, A., Joseph, S., 2007. Agronomic values of greenwastebiochar as a soil amendment. Aust.

207   J. Soil Res. 45, 629–634.

208 [4] Chen, B., Zhou, D., Zhu, L., 2008. Transitional adsorption and partition of nonpolar and polar aromatic contaminants by biochars of pine

209   needles with different pyrolytic temperatures. Environ. Sci. Technol. 42, 5137–5143.

210 [5] Chun, Y., Sheng, G.Y., Chiou, C.T., Xing, B.S., 2004. Compositions and sorptive properties of crop residue-derived chars. Environ. Sci.

211   Technol. 38, 4649–4655.

212 [6] Crombie, K., Mašek, O., Sohi, S.P., Brownsort, P., Cross, A., 2013. The effect of pyrolysis conditions on biochar stability as determined by

213   three methods. GCB Bioenergy 5, 122–131.

214 [7] Dai, L., Tan, F., Wu, B., He, M., Wang, W., Tang, X., Hu, Q., Zhang, M., 2015. Immobilization of phosphorus in cow manure during

215   hydrothermal carbonization. J. Environ. Manage. 157, 49–53.

216   [8] Droussi, Z., D'orazio, V., Provenzano, M.R., Hafidi, M., Ouatmane, A., 2009. Study of the biodegradation and transformation of olive-mill

217   residues during composting using FTIR spectroscopy and differential scanning calorimetry. J. Hazard. Mater. 164, 1281–1285.

218   [9] Funke, A., Ziegler, F., 2010. Hydrothermal carbonization of biomass: A summary anddiscussion of chemical mechanisms for process

219   engineering. Biofuels Bioprod. Bior. 4, 160–177.

220   [10] Ghanim, B.M., Pandey, D.S., Kwapinski, W., Leahy, J.J., 2016. Hydrothermal carbonisation of poultry litter: Effects of treatment

221   temperature and residence time on yields and chemical properties of hydrochars. Bioresour. Technol. 216, 373–380.

222   [11] Guo, S., Dong, X., Wu, T., Shi, F., Zhu, C., 2015. Characteristic evolution of hydrochar from hydrothermal carbonization of corn stalk. J.

223   Anal. Appl. Pyrol. 116, 1–9.

224   [12] Kei, M., Toshitatsu, M., Yasuo, H., Nishihara, K., Nakanishi, T., 2004. Removal of nitrate-nitrogen from drinking water using bamboo

225   powder charcoal. Bioresour. Technol. 95, 255–257.

226   [13] Keiluweit, M., Nico, P.S., Johnson, M.G., Kleber, M., 2010. Dynamic molecular structure of plant biomass-derived black carbon (biochar).

227   Environ. Sci. Technol. 44, 1247–1253.

228   [14]Ko, H.J., Kim, K.Y., Kim, H.T., Kim, C.N., Umeda, M., 2008. Evaluation of maturity parameters and heavy metal contents in composts

229   made from animal manure. Waste Manage. 28, 813–820.

230   [15]Lehmann, J., 2007. A handful of carbon. Nature 447, 143–144.

231   [16]Li, J., Liang, N., Jin, X., Zhou, D., Li, H., Wu, M., Pan, B., 2017. The role of ash content on bisphenol A sorption to biochars derived from

232   different agricultural wastes. Chemosphere 171, 66–73.

233   [17]Libra, J.A., Ro, K.S., Kammann, C., Funke, A., Berge, N.D., Neubauer, Y., Titirici, M.-M., Fühner, C., Bens, O., Kern, J., Emmerich, K.H.,

234   2011. Hydrothermal carbonization of biomass residuals: a comparative review of the chemistry, processes and applications of wet and dry

235   pyrolysis. Biofuels 2, 71–106.

236   [18]Makara, A., Kowalski, Z., 2015. Pig manure treatment and purification by filtration. J. Environ. Manag. 161, 317–324.

237   [19]Mohan, D., Sarswat, A., Ok, Y.S., Pittman, C.U. Jr., 2014. Organic and inorganic contaminants removal from water with biochar, a

238   renewable, low cost and sustainable adsorbent – A critical review. Bioresour. Technol. 160, 191–202.

239   [20]Ponnamperuma, F.N., 1984. Straw as a source of nutrients for wetland rice. Organic matter and rice. Manila (Philippines): International Rice

240   Research Institute, p. 117–136.

241 [21]Smith, A.M., Singh, S., Ross, A.B., 2016. Fate of inorganic material during hydrothermal carbonisation of biomass: Influence of feedstock

242 on combustion behaviour of hydrochar. Fuel 169, 135–145.

243 [22]Tan, X.F., Liu, Y.G., Zeng, G.M.,Wang, X., Hu, X.J., Gu, Y.L., Yang, Z.Z., 2015. Application of biochar for the removal of pollutants from

244 aqueous solutions. Chemosphere 125, 70–85.

245 [23]Wang, Y., Lu, H., Liu, Y., Yang, S., 2016. Ammonium citrate-modified biochar: An adsorbent for La(III) ionsfrom aqueous solution. Colloid.

246 Surface. A: Physicochem. Eng. Aspects 509, 550–563.

247 [24]Xiao, X., Chen, B., Zhu, L., 2014. Transformation, morphology, and dissolution ofsilicon and carbon in rice straw-derived biochars under

248 different pyrolytic temperatures. Environ. Sci. Technol. 48, 3411–3419.

249 [25]Zheng, C., Bluemling, B., Liu, Y., Mol, A.P.J., Chen, J., 2014. Managing manure from China's pigs and poultry: The influence of ecological

250 rationality. AMBIO 43, 661–672.

251

20

252 Table 1. Basic physical and chemical properties of bio- and hydrochars obtained from RS and PM at different temperatures.

Biochar	Yield (%)	Moisture (%)	VM* (%)	FC* (%)	H/C	O/C	(O+N)/C	C/N	pH	EC* (mS/cm)	SSA* (m²/g)	TPV* (cm³/g)	MPS* (nm)
RS-P300	57.7	6.29	45.0	24.3	1.04	0.379	0.396	56.9	7.15±0.01	4.36±0.13	3.35	0.0127	151.3
RS-P500	33.8	5.93	14.6	51.0	0.58	0.178	0.193	67.2	10.4±0.05	4.54±0.06	7.47	0.0202	108.1
RS-P700	30.7	7.15	7.40	56.6	0.37	0.083	0.097	71.3	10.6±0.09	5.89±0.16	32.9	0.0486	59.2
PM-P300	57.8	6.15	31.4	34.2	1.00	0.354	0.410	18.0	7.53±0.04	0.543±0.022	3.32	0.0191	229.9
PM-P500	42.9	4.52	14.9	40.2	0.59	0.171	0.215	22.3	7.97±0.03	0.586±0.033	6.30	0.0291	184.5
PM-P700	38.0	4.68	7.62	44.9	0.31	0.146	0.171	39.4	8.98±0.04	0.919±0.050	20.5	0.0454	88.4
RS-H180	56.0	5.73	68.9	18.8	1.47	0.735	0.746	91.4	5.69±0.08	0.062±0.005	2.57	0.0202	314.1
RS-H240	37.6	3.43	58.2	24.3	1.08	0.335	0.352	58.2	5.58±0.07	0.055±0.004	4.46	0.0382	342.5
RS-H300	25.6	3.00	52.2	26.4	0.94	0.165	0.184	51.8	5.92±0.10	0.040±0.006	2.94	0.0128	174.3
PM-H180	56.7	5.04	44.2	20.6	1.18	0.340	0.382	24.2	5.43±0.01	0.147±0.005	15.5	0.0907	233.5
PM-H240	46.8	3.37	35.8	31.3	1.04	0.264	0.309	22.1	5.76±0.05	0.092±0.003	15.6	0.1212	310.6
PM-H300	43.7	2.40	26.8	35.4	0.91	0.187	0.236	20.2	5.99±0.02	0.051±0.005	10.7	0.0728	272.7

253 * VM, volatile matter; FC, fixed carbon; EC, electric conductivity; SSA, specific surface area; TPV, total pore volume; MPS, mean pore size.
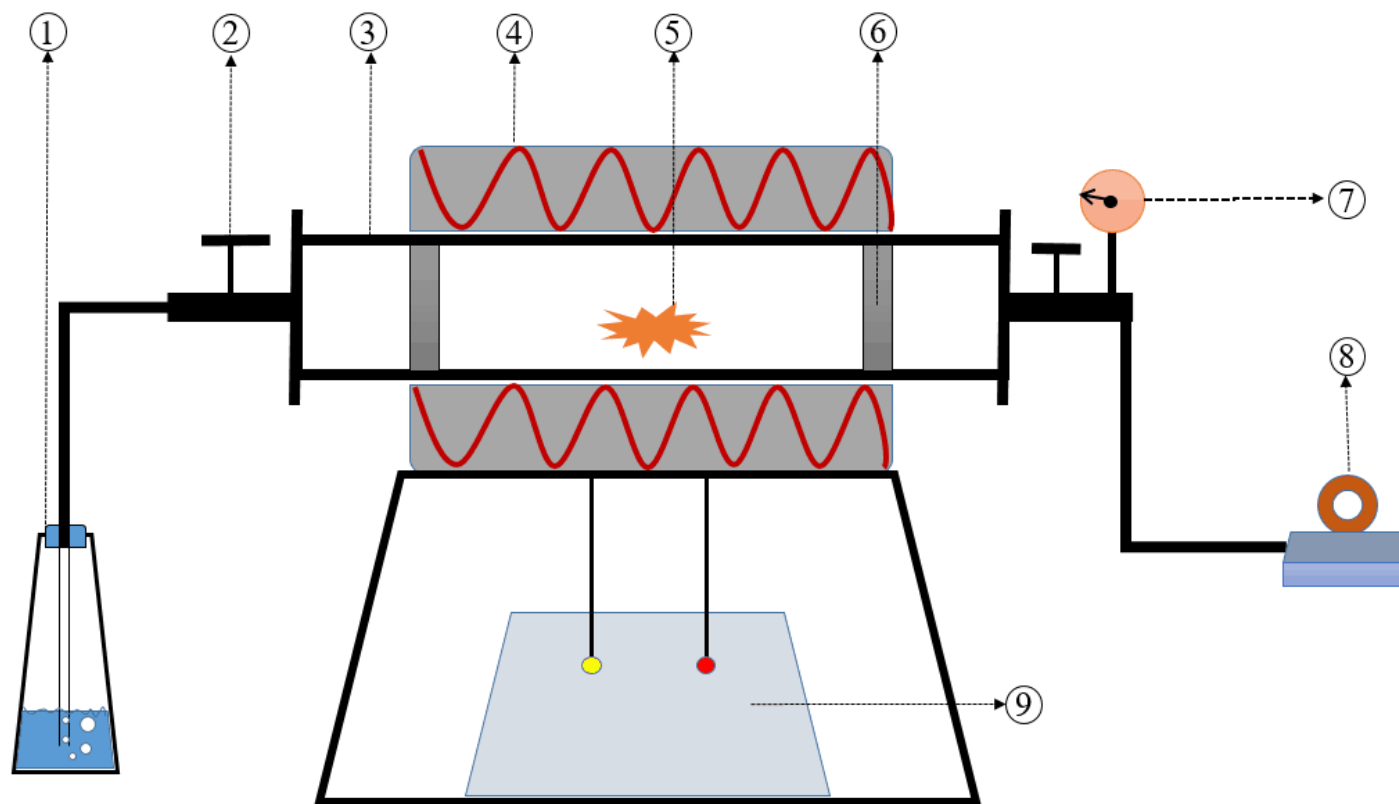
254

255 **Figure captions**

256 Fig. 1. Schematic diagram of pyrolysis setup. 1) Exhaust gas absorber; 2) valve; 3) quartz tube; 4) heating jacket; 5) biomass; 6) filter plug; 7)

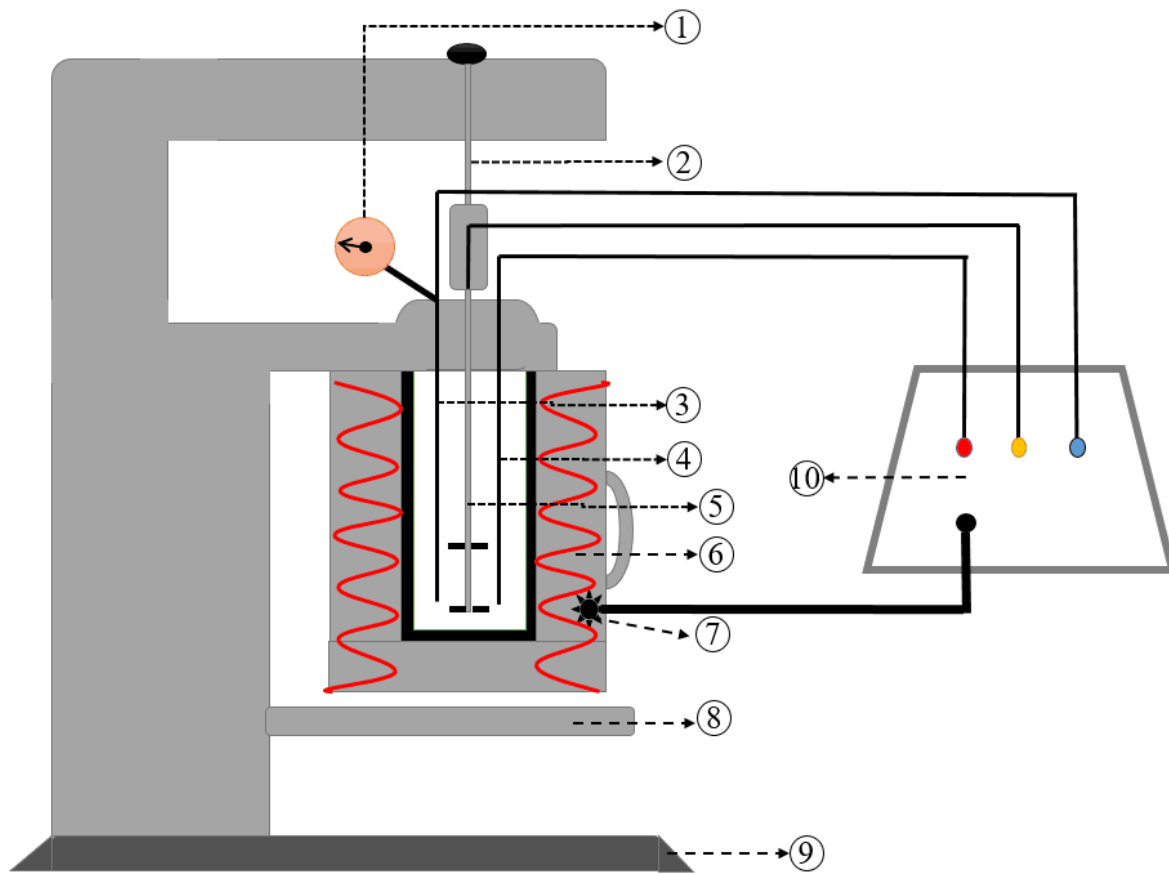257 pressure meter; 8) vacuum pump; 9) temperature controller.

258 Fig. 2. Schematic diagram of hydrothermal carbonization setup. 1) Pressure meter; 2) magnetic stirrer; 3) pressure sensor; 4) temperature sensor;

259 5) magnetic stirrer; 6) heating jacket; 7) power port; 8) protection platform; 9) support base; 10) PID controller.

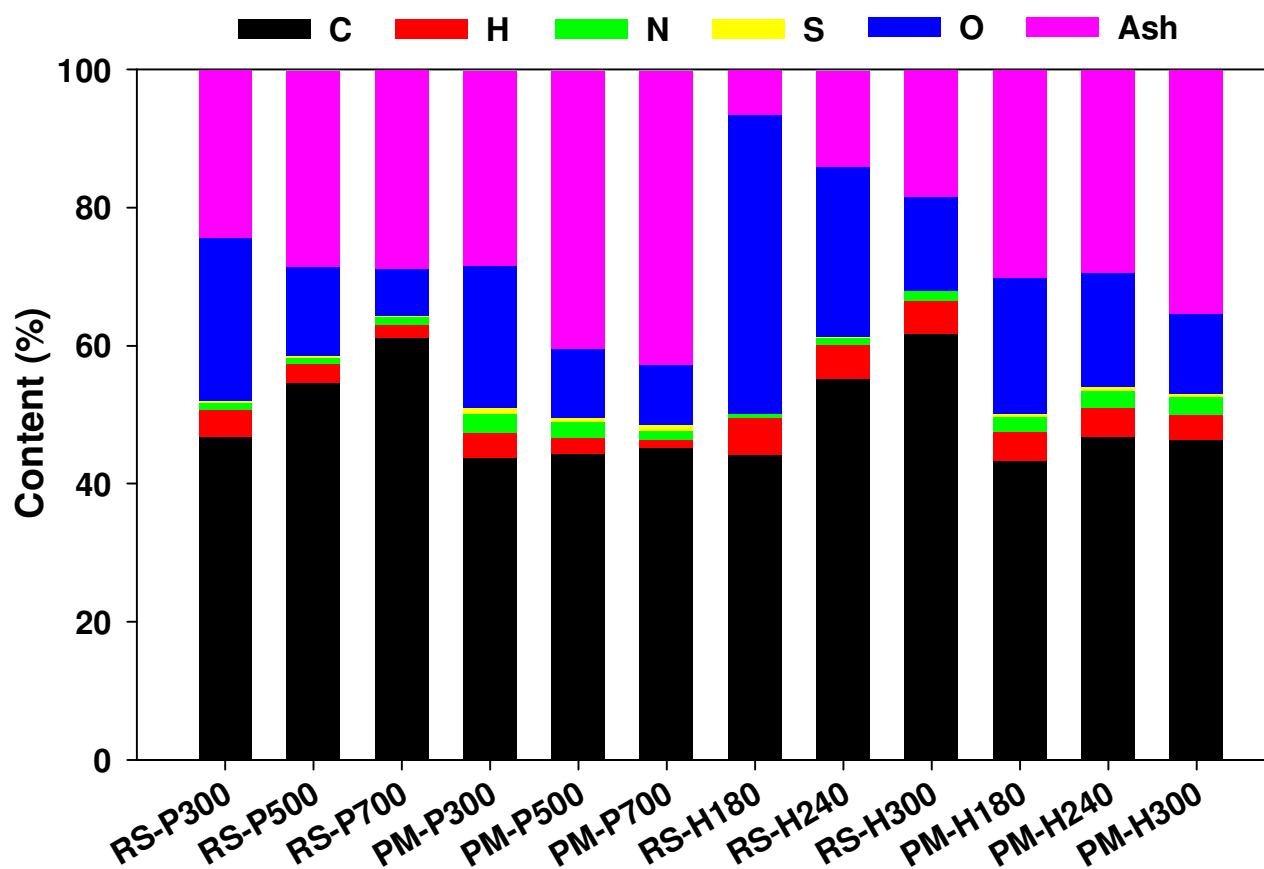260 Fig. 3. C, H, N, S, O and ash content of biochars and hydrochars.

22

261

262   Fig. 1.

263

264   Fig. 2.

265

266

267   Fig. 3.

268

269   **Highlights:**

270   • Bio- and hydrochars were obtained by thermal treatment of rice straw and pig

271   manure

272   • Higher temperatures resulted in lower bio-/hydrochar yields

273   • Biochars showed lower H/C ratios than hydrochars due to their greater stability

274   • Rice straw is suited for carbon sequestration by pyrolysis/hydrothermal

275   carbonization

276   • Pig manure is suitable for use as a soil amendment substrate

277